

VARIABILITY OF FREE TROPOSPHERIC HUMIDITY FROM METEOSAT OVER THE TROPICS: 1983-2005

Hélène Brogniez¹, Julien Lémond², Rémy Roca² and Laurence Picon²

¹Centre d'Etude des Environnements Terrestre et Planétaires IPSL/CNRS, Vélizy, France

²Laboratoire de Météorologie Dynamique IPSL/CNRS, Palaiseau, France

Abstract

The extended set of the water vapor channel observations from METEOSAT First Generation over the 1983-2005 period is converted into Free Tropospheric Humidity which describes the relative humidity averaged over the troposphere. This 23 years 3 hourly database permits to investigate the variability of the humidity over the tropical Atlantic and African areas at multiple scales: decennial, interannual, seasonal, intraseasonal and synoptic scales. The present study takes advantage of the high frequency of the observations to built significant estimates of the intraseasonal variability (~20 days). A first analysis at the seasonal scale reveals that the intraseasonal variance over the subtropical dry regions has a strong cycle in the Northern Hemisphere that is not observed in the Southern Hemisphere. Dynamical interpretation using back trajectory will be performed to document this mode of variability. A second analysis at the interannual scale, focused on the dry eastern Mediterranean region that is characterized by around 25% of normalized variance in FTH, indicates that the extreme summers are related to the complex mixing of extra tropical and tropical air that modulates the dryness of the area. Preliminary results concerning longer time scale are also discussed.

1. INTRODUCTION

The importance of free tropospheric water vapor in the determination of the climate sensitivity [e.g. *Spencer and Braswell*, 1997] has led to an increased effort to document and understand its distribution and variability, and to assess its representation in climate models [*Allan et al*, 2003; *Brogniez et al*, 2005; etc]. Measurements in the so-called "water vapor" band by radiometers such as the MVIRI imager (now SEVIRI) onboard the METEOSAT satellites since 1977 provide estimations of the humidity content of a wide layer of the free troposphere, commonly referred to as the upper tropospheric humidity (UTH) or free tropospheric humidity (FTH). Thanks to the continuous series of METEOSAT, the variability of water vapor above the Africa/tropical Atlantic region can be study from decadal down to synoptic timescales.

The next section is dedicated to the description of the FTH retrieval algorithm designed for the METEOSAT observations and to the presentation of the now available database covering the 1983-2005 period, and developed at LMD following *Picon et al* [2003] and *Brogniez et al* [2006]. Section 3 presents the interannual characteristics of the database, focusing on the summer, as well as an attempt to interpret the variability of the dry region of the Eastern Mediterranean using a dynamical tool. Finally, the main conclusions are drawn and a rapid insight of current analyses at LMD is provided.

2. DESCRIPTION OF THE DATABASE

2.1 The Free Tropospheric Humidity retrieval for METEOSAT

In clear air conditions, observations performed in the water vapor absorption band ($\sim 6.3\mu\text{m}$) may be interpreted in terms of a layer-mean relative humidity [Schmetz and Turpeinen, 1988; Soden and Bretherton, 1993; etc] through the following log-normal relationship:

$$\ln\left(\frac{\langle RH \rangle \cdot p_0}{\cos\theta}\right) = a \cdot BT_{6.3} + b \quad (1)$$

where $BT_{6.3}$ is the $6.3\mu\text{m}$ brightness temperature, θ is the satellite viewing angle, p_0 is a scaling factor related to the vertical thermal structure ($p_0 = p[T=240\text{K}] / 300\text{hPa}$), and the couple (a, b) are the fitting coefficients. Previous work [Brogniez et al., 2004] has led to introduce the local relative humidity Jacobian ($J_{RH} = \partial BT_{6.3} / \partial RH$) as the vertical averaging operator for the definition of $\langle RH \rangle$. This operator is illustrated Figure 1.a for a dry relative humidity. This illustration shows that, for this case, the operator J_{RH} is sensitive to the relative humidity of the whole free troposphere (800-100hPa).

The fitting coefficients of eq. (1) are determined using a training dataset of T and q profiles from ERA40 that are sampled over the tropical/subtropical regions. Following Brogniez et al. [2006], scenes covered with high or medium level clouds are removed from this database. For each profile, METEOSAT-5 $BT_{6.3}$ and the J_{RH} operators are computed using the RTTOV radiative code [Matricardi et al., 2004]. Finally the p_0 parameter is defined directly from the ERA40 temperature profiles to get the local thermal structure. The quality of the log-linear relationship is illustrated on Figure 1.b. This fit is characterized by a small root-mean-square error of 0.09, and a good correlation of -0.991. Hence, in the following the METEOSAT-5 $BT_{6.3}$ may be interpreted as the free tropospheric relative humidity (FTH, defined with respect to water only) using the local operator J_{RH} to define the observed layer.

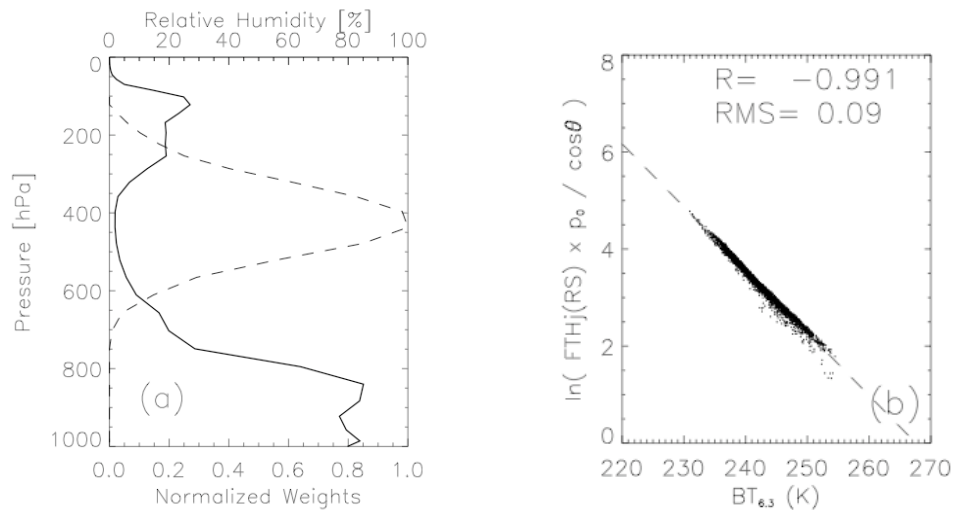


Figure 1: (a) Relative humidity profile (black line) and the corresponding relative humidity Jacobian J_{RH} (dashed line), (b) fit between the simulated $6.3\mu\text{m}$ BT and the normal-log of the J_{RH} weighted relative humidity profiles (FTH) of the training database. The dashed line represents the linear fit.

2.2 The long-term archive: 07/1983-06/2005

The METEOSAT archive regroups the complete series of the Transition Program satellites (from MET-2 to MET-7). The raw METEOSAT-2 to 7 $BT_{6.3}$ have been reprocessed at the LMD to get a homogeneous database of METEOSAT-5 "equivalent" $BT_{6.3}$ [Picon et al, 2003]. All the radiometric events (such as a change of calibration method or a change of the filter function) are taken into account in the reprocessing.

The retrieval of FTH described in § 2.1 can be applied only over clear air conditions. In addition to the pure clear sky scenes, low-level cloud pixels with top pressure greater than 680hPa are conserved in the required clear sky database since they have a negligible impact on the radiances measured in this spectral band [e.g. Brogniez *et al.*, 2006]. For the selection of both types of scenes (clear air and low-level clouds) the information provided by the DX product level of the ISCCP database are used, at the spatial and temporal resolution of the B3 pixel level: 30km every 3 hours [Rossow and Garder, 1993]. Moreover, the calibration of the METEOSAT-5 “equivalent” $BT_{6.3}$ is adjusted to the one of HIRS-12 onboard NOAA-12 following the method proposed by Bréon *et al.* [2000], which corrects a warm bias of up to 3K highlighted in the METEOSAT-5 radiances [e.g. Köpken *et al.*, 2003]. The p_0 parameter of eq. (1), needed for the retrieval of FTH, is computed using collocated temperature profiles from the ECMWF analyses (1.125°/6-hourly; ERA-40 until 2002, and the operational analyses onward). Figure 2 presents the comparison between the FTH retrieved from the METEOSAT archive following the method described above, and the FTH estimated from collocated radiosounding observations of the ECMWF archive. This comparison shows that there is a small long-term variance, highlighting a stable archive over the time span.

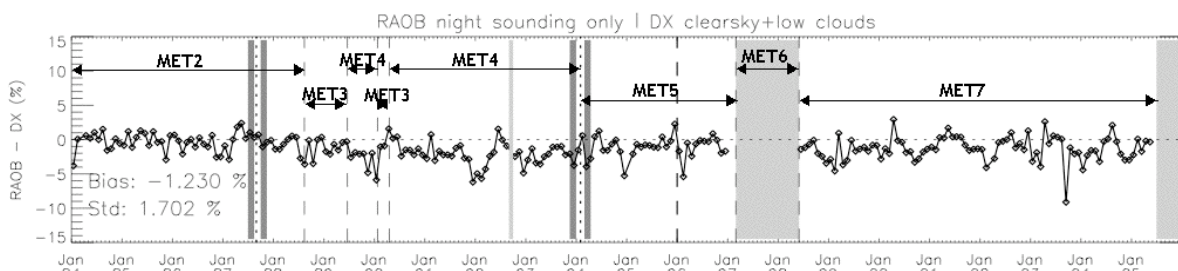


Figure 2: Comparison, in %RH, between the FTH estimated from the raob database and the retrieved FTH from the equivalent METEOSAT5 6.3 μ m BT observations. The main radiometric events of the 1984-2005 period are indicated (changes of satellite and/or of the calibration method).

3. INTERANNUAL VARIABILITY: 1984-2004

3.1 The mean seasonal cycle

The climatology of the summer season June-July-August (JJA) of the 20 complete years of the archive is presented Figure 3. The moist ITCZ is an evident pattern in the JJA mean, with the FTH reaching up to 60%. Over the subtropics (30°N/20°S), dry areas with FTH less than 10% are associated to strong subsiding motions. The interannual standard deviation (σ) of JJA highlights the high absolute variation of the ITCZ, with a maximum of σ south of the ITCZ, its mean summer position being slightly different one year to another.

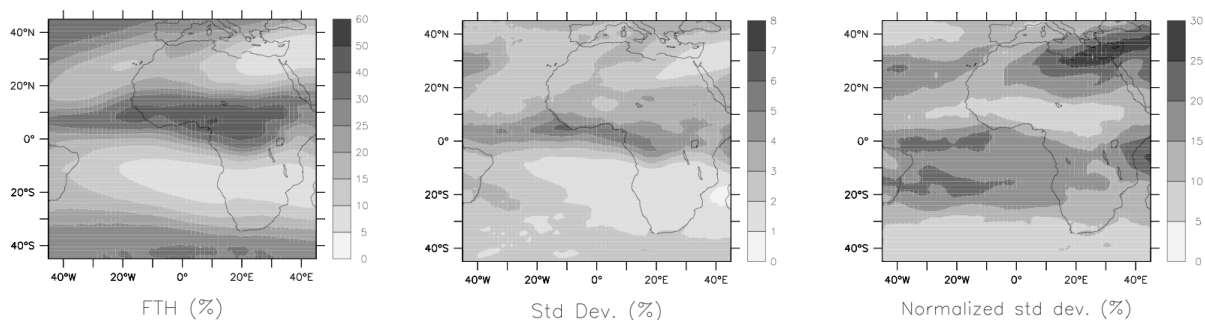


Figure 3: Climatology for June-July-August: (left) mean FTH, in %RH; (middle) interannual standard deviation σ , in %RH; (right) standard deviation normalized by the mean σ_n , in %.

The relative (normalized) standard deviation σ_n underlines the high relative variability of the driest areas and of their edges, associated to strong humidity gradients. The high values of σ_n (e.g. over the Eastern Mediterranean area) recall the role of the dry regions of the troposphere in the sensitivity of the Outgoing Longwave Radiation [Spencer and Braswell, 1997; Held and Soden, 2000].

The purpose of this study is to understand the processes that yield to the high values of σ_n in the dry regions. Thus, in the following we will focus on the Eastern Mediterranean region [20°E-30°E/25°N-35°N], which is the driest area of the METEOSAT field of observation (FTH~6%) and characterized by the highest relative variations ($\sigma_n > 25\%$).

3.2 A dynamical interpretation: example for 1992

To evaluate the atmospheric processes involved in the interannual variability of the dry regions, we reconstruct the water vapor field at 500hPa using a Lagrangian advection-condensation model [Pierrehumbert and Roca, 1998]. The point at which the air parcel last experiences saturation gives two informations: (i) the relative humidity at 500hPa at the initial position of the air parcel and (ii) the geographical location of this last saturation (latitude, longitude, pressure). This model is used like in Pierrehumbert and Roca [1998] (among others): it runs with the 6 hourly 3D wind and temperature from NCEP re-analyses, so the reconstructed field is performed 4 times a day on a 0.5° regular grid. Comparisons between the METEOSAT observed FTH and the reconstructed 500hPa RH (Figure 4) confirm that the 500hPa RH can be taken as a good proxy for the satellite FTH: the observed humidity gradient between the moist ITCZ and the dry area (FTH<10%) east of the Mediterranean Sea is indeed present in the reconstruction, as well as the amplitude of FTH.

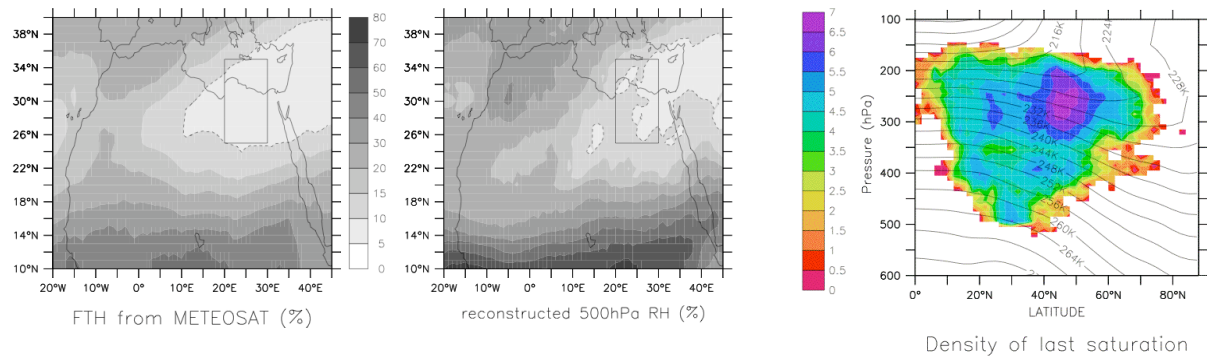


Figure 4: analysis for June-July-August 1992: (left) mean observed FTH, in %RH; (middle) mean reconstructed 500hPa relative humidity, in %RH; (right) zonally integrated distribution (in log scale, unitless) of the air masses' last saturation positions for parcels arriving over the area [20°E-30°E/25°N-35°N] during the period. The contours are the NCEP mean temperature averaged over 80°W-80°E.

The diagram on Figure 4 presents the zonal density of the distribution of the last saturation position of the air parcels that end their trajectory over the Eastern Mediterranean. This diagram highlights the complex mixing of air parcels coming from both tropical (lat<25°N) and extra-tropical (lat>25°N) regions. The main influence, for this particular summer of year 1992, seems to be extra-tropical (lat>40°N) upper tropospheric (200-300hPa) air masses, this cold (240-220K) environment bringing dry parcels to the Eastern Mediterranean. There is also an extra-tropical origin around 400hPa, associated to higher temperatures (250K) and thus moister parcels. One can also notice that there is a non-negligible quantity of air masses having a tropical (lat ~ 20°N) origin but coming from a wider layer of the troposphere (200-500hPa) associated to a generally warmer environment (260-220K), which translates into a more important supply of moisture to the area.

3.3 Towards a generalized scheme

In order to understand the interannual variability of FTH over the Eastern Mediterranean, the scheme of mixing of air masses described above is applied to the entire set of summers. Figure 5 presents a summary of this generalization, coupling the information on the latitude of origin (25°N separating the tropics and the extra-tropics) and the information on the dryness of the air parcels (limit at 10%) and cumulated over each JJA. The anomalies with respect to the mean being considered here, this diagram may be interpreted as follow: the lower-left corner concerns moist parcels (RH>10%) from extra-tropical regions (>25°N), the lower-right corner is for dry parcels from extra-tropics, the upper-left corner is for moist parcels from the tropics, and the upper-right is for dry parcels from the tropics.

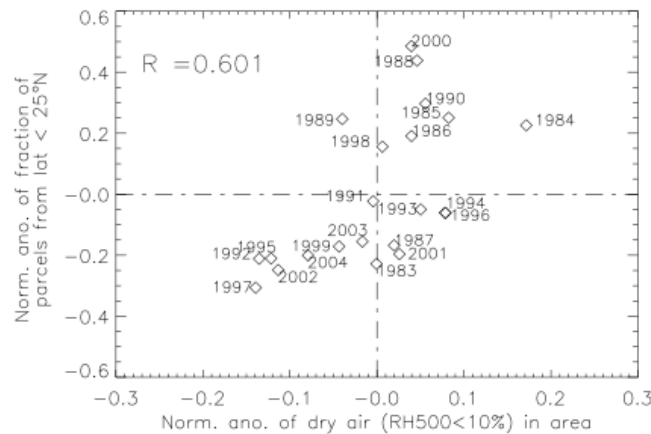


Figure 5: For the area [20°E-30°E/25°N-35°N] during each June-July-August: normalized anomaly of the fraction of air masses with a tropical last saturation position (lat < 25°N) versus the normalized anomaly of dry air (defined by RH<10%).

The value of the correlation coefficient ($R=0.6$) shows that the proposed scheme can be applied to the 20 JJA. For instance, JJA 1992 is located in the “extra-tropical and moist” part of the diagram, which fits to the description of the previous paragraph. Such interpretation may also be applied to 1997, 2002 and so on. On the other part of this diagram, one finds notably JJA 1984, noticed to be the drier summer of the period (observed FTH ~ 4.5%). According to this scheme, the dry air ending its trajectory over the Eastern Mediterranean has mainly a tropical origin.

4. CONCLUSION AND ONGOING WORKS

A 20-year database of cloud-cleared and homogeneous METEOSAT WV measurements, spanning 1983-2005, is now available and is used to perform long-term studies of the Free Tropospheric Humidity (FTH) over Africa and the tropical Atlantic region. The FTH is defined from the relative humidity profile weighted by the water vapor jacobian function. Its interannual climatology reveals a high relative variability of the driest parts of the troposphere, more particularly over the Eastern Mediterranean region, emphasizing its role in the sensitivity of the OLR. The use of a dynamical model over this dry region reveals a complex mixing of air masses having tropical (<25°N) and extra-tropical (>25°) origins, the main origin of the air masses varying amongst the 20 summers, thus explaining the interannual variability of FTH.

Extension of the present findings to the full dry areas rather than the limited Mediterranean box is currently performed. Empirical Orthogonal Functions have been computed for the dataset and reveals a first long period mode of variability that needs to be confirmed as geophysical or artifact of the time series. One of the other modes captures more than 50% of the local variability over the extended Eastern Mediterranean area and exhibits ~3 to 5 years period. Teleconnections with large scale dynamical fields are currently looked for in order to link these dry areas variability to some perturbations of the circulation.

5. REFERENCES

- Allan R. P., M. A. Ringer, and A. Slingo, (2003), Evaluation of moisture in the Hadley Center climate model using simulations of HIRS water vapour channel radiances. *Q. J. R. Meteorol. Soc.*, **129**, pp. 3371-3389.
- Bréon F-M., D. Jackson and J. Bates, (2000), Calibration of the METEOSAT water vapor channel using collocated NOAA/HIRS-12 measurements. *J. Geophys. Res.*, **105**, pp. 11,925-11,933.
- Brognez H., R. Roca and L. Picon, (2004), Interannual and Intraseasonal variabilities of the Free Tropospheric Humidity using METEOSAT water vapor channel over the tropics, *Proc. of the Eumetsat Meteorological Satellite Conference, Prague, Czech Rep.*, 31-4 June.

Brogniez H., R. Roca and L. Picon, (2005), Evaluation of the distribution of subtropical free tropospheric humidity in AMIP-2 simulations using METEOSAT water vapor channel data. *Geophys. Res. Lett.*, **32**, L19708, doi:10.1029/2005GL024341.

Brogniez H., R. Roca and L. Picon, (2006), A clear sky radiance archive from METEOSAT "water vapor" observations. *J. Geophys. Res.*, **111**, D21109, doi:10.1029/2006JD007238.

Köpken C., J-N Thépaut and G. Kelly, (2003), Assimilation of geostationary WV radiances from GOES and METEOSAT at ECMWF. EUMETSAT/ECMWF Fellowship Program, Res. Report n°14.

Held I., and B. Soden, (2000), Water vapor feedback and global warming. *Annu. Rev. Energy Environ.*, **25**, pp. 441-475.

Matricardi, M., F. Chevallier, G. Kelly and J-N Thépaut, (2004), An improved general fast radiative transfer model for the assimilation of radiance observations, *Q. J. R. Meteorol. Soc.*, **130**, pp. 153-173.

Picon L., R. Roca, S. Serrar, J-L. Monge, and M. Desbois, (2003), A new METEOSAT "water vapor" archive for climate studies. *J. Geophys. Res.*, **108**, 4301, doi:10.1029/2002JD002640.

Pierrehumbert R.T., and R. Roca, (1998), Evidence for control of Atlantic subtropical humidity by large-scale advection. *Geophys. Res. Lett.*, **24**, pp. 4537-4540.

Rossow W. and L. Garder, (1993), Validation of the ISCCP cloud detection. *J. of Climate*, **6**, pp. 2370-2393.

Schmetz J., and O. Turpeinen, (1988), Estimation of the upper tropospheric relative humidity field from METEOSAT water vapor image data. *J. of Appl. Meteor.*, **27**, pp. 889-899.

Soden B. and F. Bretherton, (1993), Upper tropospheric relative humidity from the GOES 6.7 μ m channel: Method and climatology for July 1987. *J. Geophys. Res.*, **98**, pp. 16,669-16,688.

Spencer R., and W. Braswell, (1997), How dry is the tropical free troposphere? Implications for a global warming theory. *Bull. Am. Meteor. Soc.*, **78**, pp. 1097-1106.